FACULTAT
DE CIÈNCIES, TECNOLOGIA
I ENGINYERIES
UVIC | UVIC·UCC

Treball de Fi de Grau Experimental

CARACTERITZACIÓ FUNCIONAL I COMPUTACIONAL DE MUTACIONS DELS GENS GRIN

ISMAEL VERA MUÑOZ

Grau en Biotecnologia

Tutors: Dra. Mireia Olivella García i Dr. Xavier Altafaj Tardío

Vic, juny de 2023

Acknowledgements

I want to express my thankfulness to my tutors Dra. Mireia Olivella and Dr. Xavier Altafaj for not only giving me the opportunity of joining their team, but to patiently guide me through this process.
What is more, to let me learn and participate in both sides of the project, functional experiments in the laboratory, and bioinformatic assays.

Besides, I want to thank my family and friends for supporting me while performing this project, and during the whole university degree.

Summary

Title: Functional and computational characterization of GRIN gene mutations
Author: Ismael Vera Muñoz
Supervisors: Dra. Mireia Olivella García and Dr. Xavier Altafaj Tardío
Date: Vic, June of 2023
Keywords: Glutamatergic synapse, NMDA receptor, GRIN, disease-associated mutations.

Glutamatergic synapse is crucial for synaptic plasticity, neuronal development, learning, and memory. Glutamate binds to ionotropic N-methyl-D-aspartate (NMDA) receptors, producing excitatory postsynaptic potential. Autosomal dominant or *de novo* GRIN gene variants are associated with GRIN related disorders (GRDs), rare pediatric encephalopathies caused by NMDA receptor malfunction; clinically manifested as intellectual disability, hypotonia, and epilepsy. In order to select the best strategic therapy, the variants need to be classified as loss-of-function (LoF) or gain-of-function (GoF). This experimental variant stratification is time consuming and thus computational approaches to predict variant pathigenesis and functionallity are being used.
10 GRIN *de novo* missense variants from patients without functional classification have been functionally characterized. Methods used for the functional characterization include primer design, site-directed PCR Mutagenesis, DNA precipitation, bacterial transformation, DNA extraction and quantification, Sanger sequence analysis, CalPhos and Lipofectamine transfection, western blot, and immunofluorescence. From these, 3 variants had correct composition and expression of NMDA receptor. In addition, these 10 variants have been introduced in the NMDA molecular model to see the molecular changes caused by the mutation.

Besides, in order to understand the most vulnerable regions of the NMDA receptor, and the regions related to LoF or GoF, functional and pathogenic information of all previously reported GRIN missense variants from the GRIN data base (GRINdb) and GenomAD were mapped and integrated in the already determinate triheteromeric molecular model of the NMDA receptor in PyMOL, via a computational assay based on Python scripts.
The model Results indicates that pathogenic variants mainly affect the the ligand-binding domain (LBD) and transmembrane domain (TMD), while the LBD is mostly affected by LoF variants.

Overall, these results contribute to a better understanding of how missense variants affect the structure and the function of the receptor.

Resum

Títol: Caracterització funcional i computacional de mutacions dels gens GRIN
Autor: Ismael Vera Muñoz
Tutors: Dra. Mireia Olivella García and Dr. Xavier Altafaj Tardío
Data: Vic, juny 2023
Paraules clau: sinapsi glutamatèrgica, receptor NMDA, GRIN, mutacions associades a patologia.

La sinapsi glutamatèrgica és crucial per a la plasticitat sinàptica, el desenvolupament neuronal, l'aprenentatge i la memòria. El glutamat s'uneix als receptors ionotròpics de N-metil-D-aspartat (NMDA), produint potencial postsinàptic excitador. Les variants dels gens *GRIN* autosòmiques dominants o *de novo* s'associen amb trastorns relacionats amb gens GRIN (GRD), un grup d'encefalopaties pediàtriques rares causades per un mal funcionament del receptor NMDA; clínicament es manifesta com a discapacitat intel·lectual, hipotonia i epilèpsia. Per seleccionar la millor teràpia, les variants s'han de classificar com a pèrdua de funció (LoF) o guany de funció (GoF). Aquesta estratificació de variants experimentals requereix temps i, per tant, s'utilitzen enfocaments computacionals per predir la patogènesi i la funcionalitat de les variants.
S'han caracteritzat funcionalment 10 variants GRIN de novo sense sentit de pacients sense classificació funcional. Els mètodes utilitzats per a la caracterització funcional inclouen disseny de primers, PCR mutagènesi dirigida, precipitació d'ADN, transformació bacteriana, extracció i quantificació d'ADN, anàlisi de seqüències amb Sanger, transfecció amb CalPhos i Lipofectamina, western blot i immunofluorescència. D'aquestes, 3 variants tenen la composició i l'expressió correctes del receptor NMDA. A més, aquestes 10 variants s'han introduït al model molecular NMDA per veure els canvis moleculars causats per la mutació.

D'altra banda, per tal d'entendre les regions més vulnerables del receptor NMDA i les regions relacionades amb LoF o GoF, la informació funcional i patogènica de totes les variants "missense" de GRIN previament caracteritzades a la base de dades GRIN (GRINdb) i GenomAD han estat mapejades i integrades al prèviament determinat model molecular triheteromèric del receptor NMDA a PyMOL, mitjançant un assaig computacional basat en scripts Python.
Els resultats del model indiquen que les variants patogèniques afecten principalment el domini d'unió al lligand (LBD) i el domini transmembrana (TMD), mentre que el LBD es veu afectat principalment per variants LoF.

En general, aquests resultats contribueixen a una millor comprensió de com les variants de missense afecten l'estructura i la funció del receptor.

Contents

List of tables

List of figures

1- INTRODUCTION

Glutamate is the most abundant excitatory neurotransmitter in the brain, involved in synaptic plasticity, neuronal development, knowledge, and memory (Willard & Koochekpour, 2013).

Synapses are important structures that connect neurons in the nervous system through chemical or electrical signals. Glutamatergic synapses are the main excitatory synapses in the brain, consisting of glutamate localized inside presynaptic vesicles and glutamate receptors on the postsynaptic membrane (Binder et al., 2009).
Glutamatergic synapses are involved in the creation of neural network connections during the brain and spinal cord development and mediating the cellular processes crucial for synaptic transmission and plasticity (Binder et al., 2009).

During synaptic transmission, nerve impulses are transmitted to the presynaptic terminal, depolarizing the presynaptic membrane, which leads to the influx of calcium ions (Ca2+). Then, glutamate is released into the synaptic cleft through the fusion of synaptic vesicles and presynaptic membranes at the active zone (Binder et al., 2009).

Glutamate binds to N-methyl-D-aspartate (NMDA) receptors, leading to the sodium and potassium ion permeability of the two sides of the postsynaptic membrane, producing excitatory postsynaptic potential (Binder et al., 2009).

To avoid neuronal death by abnormal high levels of glutamate, and for glutamate-mediated neurotransmission to be efficient, glutamate levels inside neurons and in the intercellular space, must be very finely regulated and maintained at adequate concentrations (Choi et al., 1987). This process is carried out by a series of transporters located in the plasmatic membrane of neurons (Gegelashvili et al., n.d.).

Glutamate receptors (GluR) are classified as ionotropic and metabotropic (Rojas et al., 2016). Metabotropic glutamatergic receptors (mGluR) modulate neuronal excitability and synaptic transmission (Gregory et al., n.d.). They do not form an ion channel pore, but use signal transduction mechanisms, such as G protein. The mGluRs include 8 receptors divided into 3 groups based on functional, structural, and transductional criteria (Kantrowitz et al., n.d.). Group I is formed by mGluR1 and mGluR5 subtypes, which are linked to Gq protein (subunit of protein G); located at presynaptic and postsynaptic neurons. Group II is composed of mGluR2 and mGluR2; group III of mGluR4, mGluR6, mGluR7 and mGluR8. Both groups II and III are linked to Gi protein (subunit of protein G) and located at presynaptic level (Gregory et al., n.d.).

Ionotropic glutamate receptors (iGluR) are transmembrane ion channels that may open or close in response to the binding of a specific molecule or a neurotransmitter. There are three types of ionotropic glutamate receptors: NMDA, AMPA, and kainate receptors. They are named based on the agonist molecule that activates them: NMDA receptors, for N-methyl-D-aspartate; AMPA receptors, for a-amino-3-hydroxyl-5-methyl-4-isoxazole-propionate; and kainate receptors, for kainic acid (Willard & Koochekpour, 2013).

NMDA, AMPA, and Kainate receptors form non-selective cation channels, permeable to both sodium (Na+) and potassium (K+) ions. So, glutamate binding causes depolarization of the postsynaptic membrane (postsynaptic excitatory potential).
Both AMPA and Kainate receptors generate excitatory postsynaptic currents that are responsible for initiating action potentials (Rivadulla et al., 2001).

NMDA (N-methyl-D-aspartate) receptor channel allows the movement of calcium ions (Ca2+), in addition to Na+ and K+, which implies a concentration increment of intracellular Ca2+ in the postsynaptic neuron, every time the receptor is activated (Schackert et al., 2023; Willard & Koochekpour, 2013). NMDA receptor requires binding to glutamate and , the presence of a co-agonist (glycine), to open the channel (Hansen et al., n.d.; Johnson et al., n.d.).
Furthermore, the channel can be blocked by magnesium ions (Mg+), when the membrane potential is close to the resting value (Hansen et al., n.d.).

NMDARs are heterotetramers mostly composed of the assembly of two glycine/D-serine-binding GluN1 subunits (encoded by GRIN1 gene) and two glutamate-binding subunits GluN2A/GluN2B (encoded by GRIN2A and GRIN2B genes, respectively) (Rojas et al., 2016).

NMDARs can also have the presence of GluN2C, GluN2D, GluN3A, and/or GluN3B subunits at particular developmental stages and in precise neuronal subtypes (Gregory et al., n.d.).
The subunit composition determines NMDAR biophysical properties. However, the receptor activity is regulated by small ions and molecules, such as protons, zinc, spermine (Kantrowitz et al., n.d.), membrane lipids (Rivadulla et al., 2001), and proteins, involved in posttranslational modifications (Schackert et al., 2023) and protein–protein interactions (Hansen et al., n.d.).

The structure of NMDAR is composed of four domains: (i) two extracellular domains that include the amino-terminal (ATD) and the ligand-binding domains (LBD), (ii) the transmembrane domain (TMD) that constitutes the channel's pore, and (iii) a cytoplasmic carboxy-terminal domain (CTD).

NMDAR's structure for both diheteromer GluN1/GluN2A (Zhang et al., n.d.) and GluN1/GluN2B (Chou et al., n.d.) has been determined.
NMDA receptors are directly related to GRIN related disorders (GRDs), which are a group of rare paediatric encephalopathies resulting from the presence of pathogenic GRIN gene variants (Santos-Gómez et al., 2020). A single mutation in GRIN genes can cause NMDAR malfunction leading to neurodevelopmental diseases, with an autosomic dominant inheritance or de novo mutations.Clinically, this neurodevelopmental condition is manifested by a spectrum of neurological and systemic alterations, including intellectual disability, hypotonia, communication impairment, epilepsy, movement and sleep disorders, and gastrointestinal disturbances (Santos-Gómez et al., 2020).

There are different types of GRIN variants related with GRDs; such as missense, protein truncating (nonsense, frameshift), amino acid insertions and deletions, large DNA insertions, deletions and translocations, and chromosomal aberration (García-Recio et al., 2021). GRIN variants pathogenicity is classified as "Disease-associated," "Neutral," or "Uncertain pathogenicity," according to their NMDAR alteration. Disease-associated variants can cause a Gain of Function (GoF) or Loss of Function (LoF). GoF variants facilitate NMDAR signalling, while LoF decrease the activity causing a hypoglutamatergic function (Soto et al., 2019). In addition, complex mutations, are though to need other gene mutations to cause a disease phenotype. Most LoF variants result from a decrease of NMDAR surface expression or a reduction of charge transfer across the mutant NMDAR. On the contrary, GoF variants are frequently associated with: reduction or abolishment of magnesium blockade, increase of agonist potency, and decrease of deactivation rate (García-Recio et al., 2021).

Disease-associated protein truncating variants (PTVs) functionally recapitulate GRIN2A and GRIN2B haploinsufficiency, as the NMDA receptor does not arrive to the cell membrane. Thus, these variants are classified as LoF variants when the truncation affects the ATD, LBD or the TMD. Despite that fact, heterozygous GRIN1 PTVs do not alter NMDAR-mediated currents (Santos-Gómez et al., 2020).

Clinical phenotype of disease-associated GRIN1 variants show in both GoF and LoF there is presence of epilepsy (57% and 56%, respectively) and developmental delay (86% and 81%, respectively). However, intellectual disability is present in all LoF variants (100%), against its absence in GoF variants (0%) (García-Recio et al., 2021).

GRIN2A phenotype shows GoF variants are more frequently associated with intellectual disability (89%) and development delay (83%), than with LoF variants (46% in both cases). Whereas speech disorder is more frequently associated with GRIN2A LoF variants (73%), than with GoF variants (50%) (García-Recio et al., 2021).

When it comes to GRIN2B, epilepsy is more common associated with GoF (83%) than with LoF variants (40%). Nevertheless, autism is present at 40% of GRIN2B LoF, on contrary to the non-presence (0%) of autism in GoF variants (García-Recio et al., 2021).

Nowadays different drugs are prescribed for NMDAR alterations. Memantine is used to treat GoF variants. Being a non-competitive NMDAR antagonist, it blocks the receptor, modulating the effects of pathological elevation of glutamate. In this way, it reduces the excitotoxicity induced by NMDAR, but still allows the activation of the receptor at physiological levels (Thomas et al., 2009). On the other hand L-serine is being used to treat LoF variants via dietary supplementation, resulting in an increment of D-serine concentration in patient's plasma. As L-serine is the substrate of serine, proving dietary supplement increases L-serine availability in the brain, promoting its conversion to D-serine, thus potentiating hypofunctional NMDARs (Soto et al., 2019).

Currently there is an increasing number of identified patients with a neurological condition carrying a GRIN variant, as the cost of exome and genome sequencing is dropping so fast. Once a patient is identified with a GRIN variant It is crucial to proceed with the stratification of the variants as pathogenic or neutral. Moreover, in order to select the best strategic therapy, a pathogenic variant should be classified as LoF or GoF.
In order to have a trustful tool to stratify faster variants and have all data countered, the GRIN database (GRINdb) was developed. GRINdb integrates all GRIN genes information in a single database, collecting data from ClinVar, genomAD, UniProt, and LOVD; it is a non-redundant, updated, and curated database gathering all available genetic, functional, and clinical data from more than 4000 GRIN variants (García-Recio et al., 2021). Moreover, in order to contribute to clinical decision-making, a structural computational algorithm was developed; based on GluN subunits' structural conservation within the NMDAR tetramer. It significantly extends the assignment of pathogenicity and functional parameters of non-annotated GRIN homologous variants.
Even though the GRINdb and the structural computational algorithm were developed, there is a large number of variants for which pathogenicity cannot be determined, so they need to be manually characterized performing functional and computational experiments (Szepetowski et al., 2022).

2- OBJECTIVES

The objectives of this research project are:

- To functionally characterize 10 GRIN variants from patients that lacks any functional classification, in order to select the most appropriate strategic therapy.
- To Integrate all the functional and pathogenic information on GRIN missense variants into the NMDA receptor structure, to understand the most vulnerable disease regions, and regions related to GoF and LoF variants.

3- METHODOLOGY

The whole laboratory process was performed at the Neurophysiology Laboratory, from the Biomedicine Department, at Universitat de Barcelona (UB).

3.1- *GRIN* MUTANTS GENERATION

For the functional characterization of 10 *GRIN de novo* variants from patients for further clinical decision-making (personalized medicine), we first generated the DNA constructs encompassing the nucleotide changes of interest. This process is composed by different steps, such as primers' design, site-directed PCR mutagenesis, DNA template digestion, DNA precipitation, bacterial transformation and amplification, DNA extraction, quantification, and Sanger sequence analysis. The variants of interest, were: GRIN1(R844C), GRIN1(D658Y), GRIN1(G638A), GRIN1(R839W), GRIN2A(G664S), GRIN2A(C456R), GRIN2B(I641T), GRIN2B(L608F), GRIN2B(F683L), and GRIN2B(D668N).

Once the variants were synthesized, they were named with the following indications: i) gene name, ii) original amino acid, iii) amino acid residue number, and iv) de novo amino acid change. For instance, "GRIN1(R844C)", changes an arginine to a cysteine at position 844 of *GRIN1* gene.

Primers design

For each variant, a forward and reverse primers were designed. A specific software from the company Agilent (*Chemical Analysis, Life Sciences, and Diagnostics | Agilent*, n.d.) was used. Once on the web page, the kit QuikChange II XL that we wanted to use was selected. The QuikChange II XL kit is used to make point mutations, replace amino acids, and delete or insert single or multiple adjacent amino acids.

Then the sequence of the gene of interest was uploaded, and the codification region was determined. Instead of that, the CDS region can also be directly uploaded. Both the sequence of the gene of interest and the CDS region are extracted from NCBI GeneBank (ncbi.nlm.nih.gov/genbank). The NCBI Reference sequences for GRIN1, GRIN2A, and GRIN2B are: NM_001270602.1, NM_012573.2, and NM_012574.1, respectively. And the coding regions: for GRIN1 from 325 to 3204, for GRIN2A from 90 to 4484, and for GRIN2B from 351 to 4799.

At this point the user can select up to 7 amino acids to change. However, as these variants are single amino acid mutations, just one site was selected. Next, the position of the mutation was selected, and at "Site 1" the new amino acid was indicated.
Once all the information is submitted, the software returns primers forward and reverse with the changed amino acid introduced.
All these primers were requested and bought at "Biomers" (biomers.net). Upon reception, the primers were resuspended in milliQ sterile water to a final 100

micromolar concentration. The data sheet for each primer provided specific information for every single primer, such as volume for resuspension, length, predicted annealing temperature and purity (MALDI analysis).

Site-directed PCR Mutagenesis

To produce high quantity of DNA with the desired amino acid change, a site-directed mutagenesis Polymerase Chain Reaction (PCR) was performed. The QuikChange II XL site-directed mutagenesis kit was employed, using PfuUltraTM high-fidelity (HF) DNA polymerase for mutagenic primer-directed replication of both plasmid strands with the highest fidelity.

First the sample reaction was prepared using the following reagents:

- 5 µL of 10x reaction buffer
- 1 µL (100 ng) of dsDNA template
- 1 µL ([125/(330*pair of bases)]*1000) of forward primer
- 1 µL ([125/(330*pair of bases)]*1000) of reverse primer
- 1 µL of dNTP mix
- 3 µL of QuikSolution
- 38 µL of pure H2O
- 1 µL of PfuUltra HF DNA Polymerase (2,5 U/µL)

These reagents have to be added starting with the largest volume to the smallest volume. And, the PfuUltra has to be added at the end of the sample preparation, once all the reagents are added. Then the samples were amplified in a thermocycler using the parameters indicated in Table 1.

Table 1: Thermocycling conditions of mutagenesis PCR

Segment	Cycles	Temperature	Time
1	1	95ºC	1 minute
2	18	95ºC	50 seconds
		60ºC	50 seconds
		68ºC	10 minutes
3	1	68ºC	7 minutes
4	1	4ºC	Holding

The different segments of cycles and temperatures allow to denature the DNA template, to anneal the mutagenic designed primers containing desired mutation, and to extend the primers with the PfuUltra DNA polymerase.

DNA template digestion

To digest the parental methylated and hemimethylated DNA, the one that does not contain the desired mutation but was used as a template in mutagenesis PCR, enzyme Dpn I was used. 1 µL of Dpn I restriction enzyme (10 U/µL) was added directly to each sample. Every mixture of the amplification reaction and the restriction enzyme was gently mixed by pipetting the solution up and down several times. Finally, the reactions were incubated at 37ºC for 2 hours to digest the parental methylated and hemimethylated DNA.

DNA precipitation

The purification and concentration of the mutated DNA was achieved throughout DNA precipitation. Briefly, the digested PCR product (50 µL) was mixed with 240 µL of EtOH 100%, 10 µL EDTA 125 mM, and 10 µL NaAc 3M. The reaction was mixed by pipetting the solution up and down several times, and incubated for 1 hour at -80ºC. After the incubation, the reaction was centrifuged at 21.000*g* at 4ºC for 30 minutes. Then the supernatant was carefully discarded using a micropipette, and the pellet was washed with 100 µL of EtOH 70%. Next, the washed pellet was centrifuged at 21.000*g* at 4ºC for 15 minutes. The supernatant was carefully discarded using a micropipette, and the pellet was dried at room temperature. Finally, the pellet was resuspended in 10 µL of pure H2O, obtaining a solution with the mutated DNA.

Bacterial transformation

To obtain a large amount of the mutated DNA, the PCR product was transformed in *E.coli* XL10-Gold ultracompetent cells, according to the manufacturer's instructions (Agilent). Briefly, competent cells were gently thaw on ice. For each sample reaction to be transformed, 45 µL of cells were transferred to individual tubes containing 2 µL of ß-mercaptoethanol. Right after, tubes were swirl and incubated on ice for 10 minutes, swirling gently the tubes every 2 minutes. Once the incubation was completed, 2 µL of the solution resulting from the DNA precipitation step, was added to the separate aliquots of the cells and incubated on ice for 30 min. DNA transformation was achieved by heat-shock, heat-pulsing the tubes at 42ºC for 45 seconds, and then incubating on ice for 2 minutes. This step allows to open the bacterial membrane, let the mutated DNA enter inside the cell, and then once on ice close the bacterial membrane again.

To make the cells start replicating, 0,5 mL of pre-heated LB medium was added to each tube, and then incubated at 37ºC for 1 hour with shaking at 250 rpm.

After the 1 hour incubation of the samples with 0,5 mL of LB, the whole volume was plated on pre-heated LB-agar plaques containing ampicillin (500 mg/L) and incubated at 37ºC overnight (O/N). From the O/N culture, bacterial colonies were picked and inoculated in a volume of 1 mL of LB+ampicillin (6 hours) and supplemented with additional 5 ml for O/N culture.

DNA extraction

The extraction of plasmid DNA was performed using an alkaline lysis-based miniprep protocol (Macherey-Nagel NucleoSpin Plasmid Purification kit; mn-net.com). Briefly, 4 mL of the bacterial o/n culture were centrifuged at 11000*g* during 30 seconds. Then, the supernatants were discarded, and 250 µL of resuspension buffer (A1) was added to each sample. Next 250 µL of lysis buffer (A2) were added, reactions were mixed by inverting the tubes 5 times, and incubated at room temperature during 5 minutes and 350 uL of neutralization buffer (A3) were added and gently mixed. The samples were centrifuged at 16000*g* for 10 minutes, and the supernatant of each sample was loaded in the miniprep column, and centrifuged at 11000*g* for 1 minute. The flow-through was discarded, and 500 µL of buffer AW were added to wash the silica membrane. Keeping on with a centrifuge of 11000*g* during 1 minute, and discarding the flow-through, 600 µL of buffer A4 were added to the sampled and centrifuged again at 11000*g* for 1 minute.

In order to dry the silica membrane, two rounds of centrifuges of 11000*g* during 2 minutes were carried out.

To finally obtain the desired DNA, 50 µL of buffer AE were carefully added directly to the silica membrane, and letting the samples incubate at room temperature for 1 minute. Following the incubation, a final centrifuge was performed at 11000*g* during 1 minute, to obtain our DNA in the flow-through.

The final flow-through was transferred to a new and sterile tube and kept at -20ºC.

DNA quantification

To proceed with further experiments it is essential to determine the concentration of the DNA we are working with. To do that, a Thermo Scientific™ NanoDrop was used not only to determine the DNA quantity, but to know the purity of the sample. This Thermo Scientific NanoDrop is a microvolume spectrophotometer that accurately measures concentration and purity from 1 µL nucleic acid or protein. The spectrophotometer measured DNA concentration of each sample in an spectrum of 260nm, and calculated the purity ratios at A260/A280 nm and A260/A230 nm.

Sequence analysis

In order to know if the desired point mutation was introduced, the final DNA sequence was analysed using Sanger sequencing. The analysis was performed at Genomics Core Facility from Universitat Pompeu Fabra. Samples needed to be prepared for the analysis, so a sequencing PCR was carried out.

For each sample was added into an Eppendorf tube:

- 0,25 µL of BigDye
- 2 µL of DNA sequencing buffer 5x
- 0,32 µL of primer
- * ng of DNA

- Pure water up to 12 µL of final volume

The primer used had to be one which annealed to the sequence 100 base-pairs (5' or 3') from the mutated nucleotide. Primers employed were previously used at the host laboratory. Primers used are shown in Table 3.

* The amount of DNA has to be previously calculated following the formula:
(25ng*(size in Kb of whole plasmid)]/DNA concentration) = DNA quantity to be added.
Once all the reactions were prepared, they were amplified in a thermocycler using the parameters indicated in Table 2.

Table 2: Thermocycling conditions of sequencing PCR

Segment	**Cycles**	**Temperature**	**Time**
1	1	94ºC	3 minutes
2	40	96ºC	10 seconds
		50ºC	5 seconds
		60ºC	4 minute
3	1	4ºC	Holding

To check if the desired point mutation was introduced, results from Sanger sequencing were analysed using software 4 peaks (nucleobytes.com/4peaks), and BLAST (blast.ncbi.nlm.nih.gov/Blast.cgi). 4Peaks is used to view and edit sequence trace files, which allowed us to check the whole sequence seeking for mutations.

Moreover, the sequences were uploaded to BLAST where they were compared and aligned with reference sequences, so as to visually see if the point mutations were introduced or not.

Table 3: Primers used for each mutant.

Mutant	**Primer used**
GRIN1(R844C)	GluN1P805Lfor
GRIN2A(G664S)	GluN2AH595RFS*28for
GRIN2A(C456R)	GluN2AH595RFS*28rev
GRIN2B(I641T)	GluN2BW559Rfor
GRIN2B(L608F)	GluN2BT532Afor
GRIN2B(F683L)	GluN2BT532Afor

3.2- CalPhos TRANSFECTION

This procedure was used for introducing DNA into mammalian cells, forming a calcium phosphate-DNA precipitate. The whole procedure lasted 3 days.

Day 1: Transfection

First of all, 1 hour before starting the transfection, the cell media was changed and replaced by DMEM medium containing 0,5 mM of D-AP5. Then, two mixtures were prepared. One containing the DNA, and another one containing the transfection buffer. Proportions for the mixture are indicated in Table 4, according to the type of plaque in which the transfection is performed.

Table 4: Quantities for CalPhos transfection mix

Plaque Multi-well 12		**Plaque Multi-well 24**	
x1 mix A	**x1 mix B**	**x1 mix A**	**x1 mix B**
1,25 µg DNA	50 µl HBS 2x	0,5 µg DNA	20 µl HBS 2x
6,25 µL CaCl 2M		2,5 µL CaCl 2M	
X µL pure H2O		X µL pure H2O	
Final volume: 50 µl		Final volume: 20 µl	

In order to mix them, first the DNA's mix (mix A) was vortexed. Then, while HBS 2x (mix B) was being vortexed, mix A was being added to mix B drop by drop.

Then the global mixture was incubated from 10 to 20 minutes at room temperature.

After the incubation, the mix was carefully added directly to the cells, ensuring to spread it around the whole plaque.

Finally, cells were incubated overnight at 37ºC and 5% of CO2.

Day 2: Medium change

Next day, after overnight incubation, the medium must be changed.

First the old medium was removed, and cells were cleaned with 10 mL of phosphate buffered saline (PBS) 1x.

Then a new medium with nutrients (complete medium) was added, as well as AP5, and cells were incubated again overnight at 37ºC and 5% of CO2.

Day 3: Fixation of cells and cell lysis

Protein extraction: to extract protein produced from the cells, the old medium was removed, and cells were washed with PBS 1x. Then RIPA buffer was added, which is a lysis buffer used for rapid, efficient cell lysis and solubilization of proteins. In a p100 plaque, the quantity of RIPA buffer to be added is from 300 to 400 µL, and in a 6 multi-well plaque from 150 to 200 µL. Then cells were gently scratched, kept in an Eppendorf tube, and incubated 15 minutes on ice. After the incubation, cells were

centrifuged at the highest possible speed during 20 minutes. The resultant supernatant was discarded, and the pellet was kept at -80ºC.

3.3- LIPOFECTAMINE TRANSFECTION

Another type of transfection was performed using lipofectamine.

In this case, the first step was to remove the medium of the cells and replace it with DMEM without Fetal Bovine Serum (FBS) and antibodies.

Then two mixes were prepared, one with DNA, and another with lipofectamine. The quantity of each mixture depends on the used plaque, and its indicated in the table below (Table 5)

Table 5: Quantities for lipofectamine transfection mix

24 Multi-well plaque	Mix A	0,8 µg DNA	50 µL DMEM	Final volume: 100 µL
	Mix B	1 µL Lipo 2000	50 µL DMEM	

The lipofectamine mixture (mix B) was the first one to be prepared, because it needs an incubation of 5 minutes at room temperature, and while it was incubating, the DNA mixture (mix A) was prepared.

Once both mixes were prepared, mix B was added to mix A and softly mixed by pipetting up and down several times. Then the global mixture was incubated during 20 minutes at room temperature. After the incubation, the reaction was added directly to the cells spreading the solution around the whole plaque, and cells were incubated at 37ºC and 5% of CO2 during 4 hours.

Next, cells' medium was removed, they were washed with DMEM, and new complete DMEM medium containing 0,2 mM of AP5 for cells transfected with GluN2A, and 0,5 mM of AP5 for GluN2B, was added.

Finally, cells were incubated overnight at 37ºC and 5% of CO2.

3.4- WESTERN BLOT

A western blot is based on the electrophoretic separation of proteins from a complex mixture according to their mass, the transfer of these proteins to a solid matrix, and the detection of specific proteins of interest on the matrix using antibodies.

First of all, an SDS-PAGE gel was prepared. Then, each sample was loaded into the gel, in equal amounts.

Once the protein samples were loaded, electrophoresis was performed at 100V for 30 minutes. During this time proteins separated according to size, with smaller proteins migrating more quickly through the gel.

When the gel electrophoresis had ended, the transfer buffer and the membrane were prepared. The transfer sandwich system with the gel close to the cathode and the

membrane near the anode was assembled. The negatively charged proteins migrated out of the gel into the membrane, when a electrophoresis at 100V during 1 hour was performed.
The following step was the immunodetection, in which antibodies are attached to the proteins. Before that, the sample was stained being with Ponceau staining 3 minutes in slow agitation. After that, the membrane was immersed 5 minutes with slow shaking into TBS Tween.
TBS tween had been previously made using for 1L of TBSTween: 100 mL of TBS, 900 mL of pure water, and 1 mL of Tween.
As the solid membrane has a high affinity for proteins, antibodies applied to the membrane can adhere to it non-specifically. To prevent this background binding, and to improve the detection step, the membrane must be blocked prior to antibody incubation. So the membrane was blocked, being 1 hour with slow shaking with blocking solution (100 mL TBSTween + 10g of 10% milk powder).
After the membrane was blocked, and the blocking solution was removed, a solution containing the primary antibody was added and incubated at 4ºC with slow shaking overnight.

The primary antibodies used are: α-HA mouse (Covance Inc., Princeton, NJ, USA) for GRIN1, and α-GFP (Clontech, France) mouse for GRIN2A and GRIN2B. Both in concentration 1:1000.
The solution containing the primary antibody was made with TBST, 5% of 10% milk powder, and 1:1000 primary antibody concentration; it has to be as large as to cover the membrane.
After the overnight incubation with the primary antibody, the membrane was washed 4 times with 10 mL of TBST. The first one is a quick wash in which TBST is added and removed; the second wash lasts 5 minutes; the third one 10 minutes; and the fourth one 15 minutes.
Then the secondary antibody was added. In this case, both GRIN1 and GRIN2A/2B use the same α-IgG mouse HRP (Life Technologies, Carlsbad, CA, USA) in 1:2000 concentration.
A solution containing the secondary antibody was also prepared with the same proportions as the solution containing the primary antibody. This solution was added to the membrane and incubated at room temperature for 1 hour with slow shaking.
Once the incubation had been completed, again the membrane was washed 4 times with 10 mL of TBST (1-5-10-15 min). Upon washing, the membranes were incubated with ECL reagent (Amersham) and chemiluminescence was detected (Chemidoc, BioRad).

3.5- IMMUNOFLUORESCENCE

Immunofluorescence is a technique using a fluorescence microscope based on the specificity of antibodies to their antigen to target fluorescent dyes. They will allow to see if NMDAR is present or not in the cells.

To start the procedure, cells were blocked by adding 400 µL of 10% FBS diluted in PBS 1x, and incubated for 1 hour with slow shaking at room temperature. After incubation, the solution was removed, and cells were cleaned with PBS 1x.

Right after, two different solutions containing one the primary antibody, and the other one containing the secondary antibody were prepared. Antibodies were the same ones as used in the western blot. These solutions contain the antibodies in FBS 1%, diluted in PBS 1x.

To keep on with the procedure, 250 µL of the solution containing the primary antibody were added to the cells, and incubated for 1 hour with slow shaking at room temperature. Then 4 washes were executed: 1 quick wash, and 3 washes of 5 minutes each one, leaving the cells in slow shaking. After the last wash of the primary antibody, 250 µL of the solution containing the secondary antibody were added to the cells, and incubating for 45 minutes with slow shaking at room temperature. Again, 4 washes were executed: 1 quick wash, and 3 washes of 5 minutes each one, leaving the cells in slow shaking. At this point having incubated both primary and secondary antibodies was time to the immunofluorescence set up.

First the laboratory slides were cleaned up with EtOH, and dried at room temperature.

Then 10 µL of DAPI, a fluorescent marker, was added to the laboratory slide. Carefully, the coverslips containing the cells were deposited on the DAPI drop, ensuring that cells were in contact with DAPI (Molecular Probes). Finally, the slides were left in a dark box overnight so as to the coverslip got perfectly attached to the laboratory slide. Microscopy images were obtained using a Nikon Eclipse 80i micro- scope (63×/1.4 N.A. immersion oil objective).

3.6- IN SILICO MAPPING OF GRIN MISSENSE VARIANTS INTO THE NMDA STRUCTURE

To create the initial molecular model for NMDA structure, a molecular model for the triheteromeric NMDA receptor (GluN1)2-GluN2A-GluN2B was generated from 4PE5 X-ray crystal structure (Karakas & Furukawa, 2014). Modeller 9.20 (Webb & Sali, 2016) was used to model the lacking regions of the receptor and Scwrl4 (Krivov et al., 2009) to position the undetermined side chains (García-Recio et al., 2021).

The molecular model includes ATD, LBD, and TMD. However, the CTD was not modelled, as there is not an available determined structure (García-Recio et al., 2021).

The 10 GRIN *de novo* variants from 10 patients were mapped in the NMDA receptor structure using PyMOL (Lunin et al., n.d.) Specifically, variants GRIN1(D658Y), GRIN1(G638A), GRIN1(R839W), GRIN2A(G664S), GRIN2A(C456R), GRIN2B(I641T),

GRIN2B(L608F), GRIN2B(F683L), and GRIN2B(D668N) were modeled in the NMDA receptor structure to see the effect of the variant in the receptor structure and function.. ariant GRIN1(R844C) could not be mapped as this position in in the intracellular domain that lacks any determined structure.

3.7- MOLECULAR MAPPING OF NMDA RECEPTOR MUTANTS

In order to identify the most pathogenic regions in the NMDA receptor and the regions that are more prone to result in a LoF or GoF, all missense variants were downloaded from Gnomad and GRINdb and were mapped to the NMDA receptor structure. Python3 (Rossum & Drake, 2009) was used to create a PyMOL (Lunin et al., n.d.) script that automatically maps all variants to the NMDA receptor structure.

Link to GitHub containing python scripts is available at supplementary material.

3.8- ETHICAL STATEMENT

Genetic reports and clinical information from individuals were provided by referring physicians. All legal guardians provided informed written consent for genetic testing in accordance with the Declaration of Helsinki and the protocol was approved by the local Ethics Committees of the participating study centers.

4- RESULTS AND DISCUSSION

4.1- Generation of *GRIN* variants constructs

In order to experimentally evaluate the functional consequences of missense variants, a collection of *GRIN* constructs harbouring the mutations of interest was first generated. To this end, a site-directed mutagenesis PCR followed by DNA digestion, bacterial transformation, DNA extraction and Sanger sequencing was performed. The DNA sequences were aligned with Blast, to identify the insertion of the missense nucleotide change of interest.

After performing the whole mutagenesis process, the desired amino acid changes were visible after the analysis with 4Peaks and Blast, resolving that 6 out of the 10 desired variants were accomplished.

The accomplished variants were GRIN1(R844C), GRIN2A(G664S), GRIN2A(C456R), GRIN2B(I641T), GRIN2B(L608F), and GRIN2B(F683L).

For all of them the change was visualized using a BLAST alignment compared to the original sequence. Also employing a 4Peaks chromatogram to graphically see the mutation.
For instance, the GRIN variant construct GRIN2A(G664S) reported an amino acid change at position 664 in both a BLAST alignment , and in the 4Peaks chromatogram (Figure 1). Indicating the expected change was correctly introduced.

<table>
<tr><th colspan="2">GRIN2A(G664S) amino acid change</th></tr>
<tr><td>(A) BLAST alignment</td><td>(B) 4Peaks chromatogram</td></tr>
<tr><td> 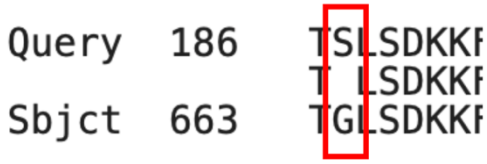
</td><td> 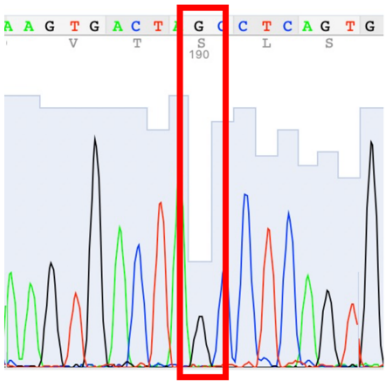 </td></tr>
</table>

Figure 1: Alignment and chromatogram of GRIN variants constructs. (A): BLAST alignment. (B): 4Peaks chromatogram. GRIN2A(G664S) variant results showing correct insertion of desired mutation.

Unfortunately, not all the designed constructs (i.e. GRIN1(D658Y), GRIN1(G638A), GRIN1(R839W), and GRIN2B(D668N)) were successfully generated, due to different technical issues.
For the GRIN1(G638A) and GRIN1(R839W) variants, after the bacterial transformation, no colonies grew on Petri dishes.
Trying to obtain cell growth, the whole procedure starting up from the mutagenesis PCR was repeated several times increasing the DNA concentration that was introduced to the bacteria. However, after the numerous attempts to obtain cell growth, no colonies grew.
On the other hand, for the GRIN2B(D668N) and GRIN1(D658Y) variants, the whole procedure worked well. In spite of that, after analysing the resultant DNA via SANGER sequencing, the mutation was not introduced, and the sequences had no changes.

As just 6 out of 10 variants were well synthesized, and the resting 4 did not acquire the mutation or did not grow colonies, different assays could be tested in a hypothetical future.
Primers could be newly designed, and the transfection protocol could be lightly modified in order to increment not only the proliferation capacity of cells, but the effectivity of transfection.

The global result of the generation of GRIN variants constructs is exposed at table 6.
For the *GRIN* variants constructs that the Sanger sequencing showed the change was correctly inserted, an additional bacterial transformation step was performed.
DH5a cells were transformed using the correct DNA from each construct. These new transformed cells were also analyzed via Sanger sequencing, and those having the correct amino acid change were used to keep a DNA stock.

Table 6: Global result of *GRIN* variants constructs generation.

MUTANT	XL1-GOLD			DH5a		
	STATUS	CLON	ID PCR seq	STATUS	CLON	ID PCR seq
GRIN2B						
GRIN2B(I641T)	Correct	1	18			
GRIN2B(L608F)	Correct	1	13	Correct	Unique	23
GRIN2B(F683L)	Correct	2	10	Correct	1	28
GRIN2B(D668N)	Incorrect	No aa change				
GRIN2A						
GRIN2A(G664S)	Correct	1	11	Incorrecte	Wrong sequence	
GRIN2A(C456R)	Correct	2	27			
GRIN1						
GRIN1(R844C)	Correct	7µL	8	Incorrecte	Wrong sequence	
GRIN1(D658Y)	Incorrect	No aa change				
GRIN1(G638A)	Incorrect	No cell growth				
GRIN1(R839W)	Incorrect	No cell growth				

Note: Accomplished steps are represented in green, and erroneous steps in red.

4.2- Functional evaluation of GluN subunits variants expression in cell lines

Just a single amino acid in *GRIN* genes might affect the even the correct formation and expression at the cell surface of mutant NMDARs. To test whether the generated constructs had a correct expression of the affected GluN subunit we underwent the expression of mutants in mammalian cell lines via CalPhos and Lipofectamine transfection.

The protein stability of GluN subunits encoded by Variants GRIN2B(L608F), GRIN2B(F683L), and GRIN1(R844C) was tested via western blot, to check protein expression; so as to know if the two subunits of the NMDA receptor are present, or there has been a malformation in them.

Controls 1 and 2 (Figure 2) show the correct presence of tagged subunits HA-GluN1 (~105 kDa) and GFP-GluN2B (~190 kDa). The three variants show a clear band at 105 kDa, indicating correct presence of subunit GluN1. However, there is a soft band at 190 kDa, meaning there is much less presence of subunit GluN2B; compared to the intense bands of GluN2B controls.
From the western blot it can be concluded the correct presence of subunit GluN1 in all 3 variants, whereas a minor presence of subunit GluN2B.

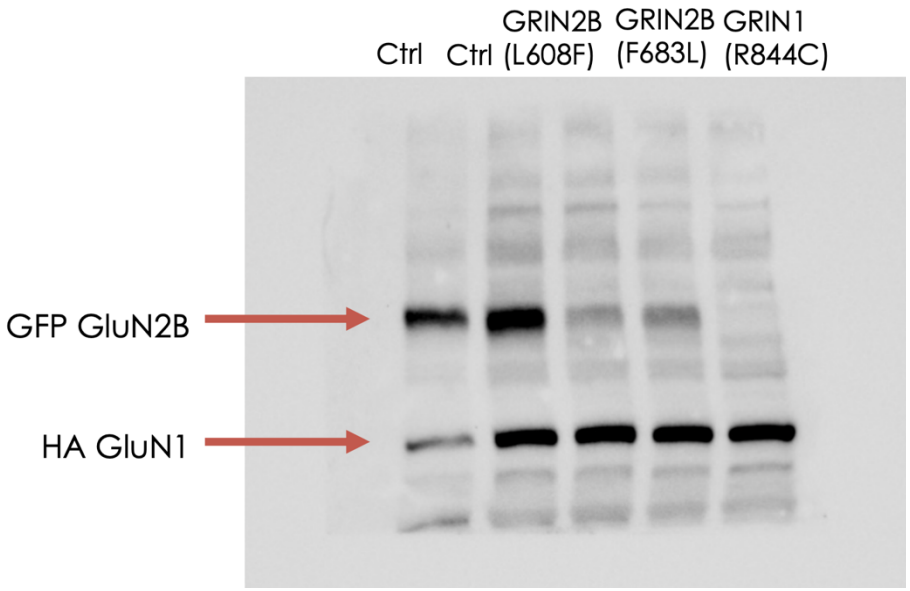

Figure 2: Western blot assay of variants GRIN2B(L608F), GRIN2B(F683L), and GRIN1(R844C). Correct presence of subunit HA-GluN1 can be appreciated at ~105 kDa, and a slight presence of subunit GFP-GluN2B at ~190 kDa.

Second, we evaluated whether the variants Variants GRIN2B(L608F), GRIN2B(F683L), and GRIN1(R844C), previously tested by western blot, reached the plasma membrane

properly or had some trafficking alterations. This aspect was addressed using immunofluorescence technique.
In transfected cells, under non-permeabilizing conditions primary antibodies, cells were blocked and incubated with primary antibodies α-HA mouse (Covance Inc., Princeton, NJ, USA) for GRIN1 and α-GFP (Clontech, France) mouse for GRIN2B, and secondary antibody α-IgG mouse HRP (Life Technologies, Carlsbad, CA, USA).

The results showed that control GFP-GluN2B wild type (Figure 3) shows the correct NMDA presence in cell surface, indicated in a bright red colour around cell membrane.
In the three analyzed variants, a defined red line can be appreciated surrounding the cell. Thus, resulting in the correct presence of the NMDA receptor in cell surface.
Red light is also emitted at the inner part of the cell, as the membrane was not permeabilized, so as to allow the expression of the receptor in the membrane.

From the immunofluorescence assay it can be resolved the correct presence of NMDA receptor in cell surface in variants GRIN2B(L608F), GRIN2B(F683L), and GRIN1(R844C).

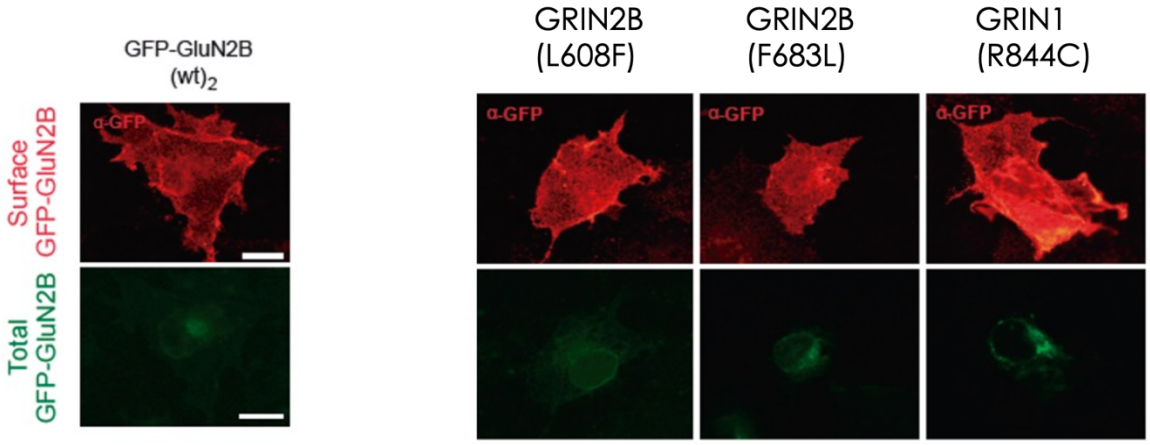

Figure 3: Immunofluorescence assay of variants GRIN2B(L608F), GRIN2B(F683L), and GRIN1(R844C). Red line around cell membrane can be appreciated, indicating a correct NMDA receptor surface expression.

Bearing in mind both western blot and immunofluorescence results, these preliminary experiments showed that variants GRIN2B(L608F), GRIN2B(F683L), and GRIN1(R844C), all have correct formation and expression of NMDA receptor.
That means even though in the western blot there is a soft band for GluN2B subunit, the receptor is correctly formed with the two subunits GluN1 and GluN2B.

Considering that resolution, it ends up in a questionable result of the western blot.
The soft band at GluN2B subunit could be caused because by problems while performing the western blot. Notwithstanding, the western blot assay should be repeated to obtain a clear and trustful outcome.

It has to be mentioned that even though the immunofluorescence assay was performed to see surface expression of the NMDA receptor, as the membrane was not permeabilized because the receptor is naturally expressed in the membrane; there can be red light emitted in the interior of the cells presence of NMDA receptor.
If the membrane is not permeabilized, NMDA receptors that are just synthesized and have not been able to reach the membrane can be also seen emitting red light.

In addition, due to the limited period of time the functional evaluation of GluN subunits variants expression in cell lines could be just performed in the three variants, GRIN2B(L608F), GRIN2B(F683L), and GRIN1(R844C).

4.3- In silico mapping of GRIN missense variants into the NMDA structure

Once having analyzed the *GRIN* variants constructs in the laboratory, these were integrated in the triheteromeric molecular model of the NMDA receptor (GluN1)2-GluN2A-GluN2B, in order to understand what the amino acid change was producing to the NMDA receptor.

Despite all the variants have been correctly indicated in the molecular model, the construct GRIN1(R844C) has not been showed, as the position 844 of GRIN1 is in the intracellular domain, that has not been determined. Figure 4 shows an overall structure of the NMDA receptor with the position of the missense variants.

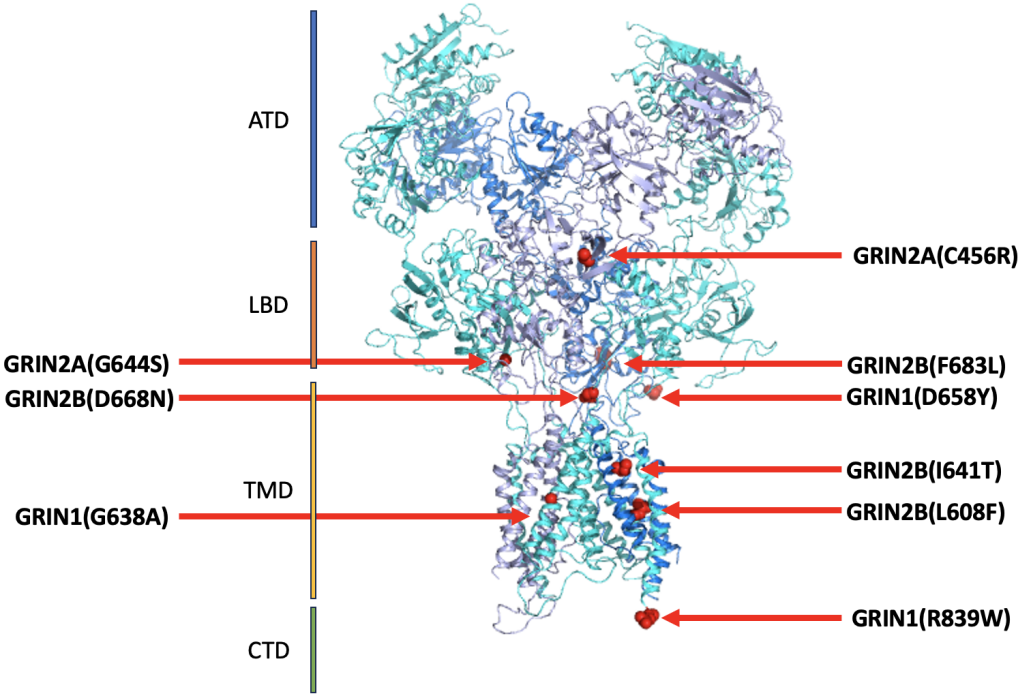

Figure 4: Studied variants represented in NMDAr molecular model. GRIN1 coloured in cyan, GRIN2A in light-blue, and GRIN2B in marine.

In order to understand how every single amino acid change can affect the NMDA receptor structure, the variants were introduced in NMDA receptor model.In addition, to know if the mutation implies more or less number of interactions with other residues, the interaction of the initial and mutated amino acids within 4Å, was also studied, figures are exposed at supplementary material.

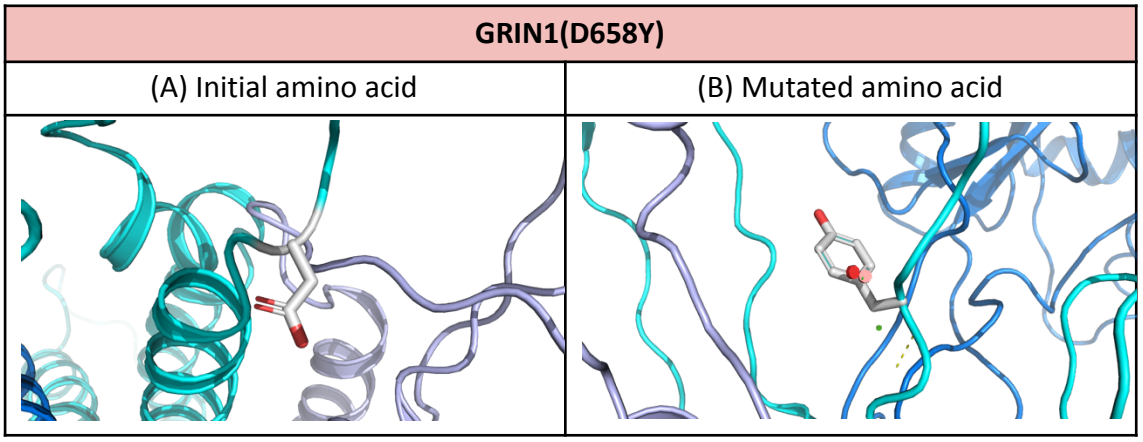

Figure 5: GRIN1(D658Y) variant in NMDA receptor molecular model. (A): Initial amino acid. (B): Mutated amino acid. GRIN1 is coloured in cyan, GRIN2A in light-blue, and GRIN2B in marine.

First variant GRIN1(D658Y) is located in the transmembrane domain.
As there is a change from a aspartic acid to a tyrosine (Figure 5), which is a neutral aromatic amino acid, there is more space occupied by the side chain of the mutated amino acid. This fact could cause even that the receptor could not fold correctly, or interfere in the blockage of magnesium, thus casuing a NMDAr malfunction.

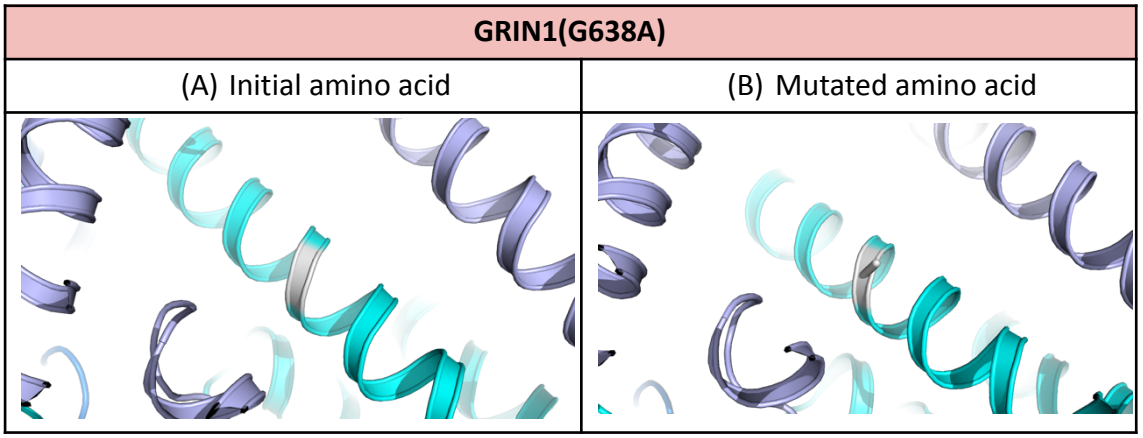

Figure 6: GRIN1(G638A) variant in NMDA receptor molecular model. (A): Initial amino acid. (B): Mutated amino acid. GRIN1 is coloured in cyan, GRIN2A in light-blue, and GRIN2B in marine.

Variant GRIN1(G638A) changes a glycine for an alanine (Figure 6), which are both neutral apolar amino acids. As alanine has a really close structure to glycine, they both interact with the same atoms within 4Å. Even this is a really small change which could not have a crucial impact in the receptor's function, in fact as it is located in the transmembrane domain, it could cause a problem in the receptor formation process.

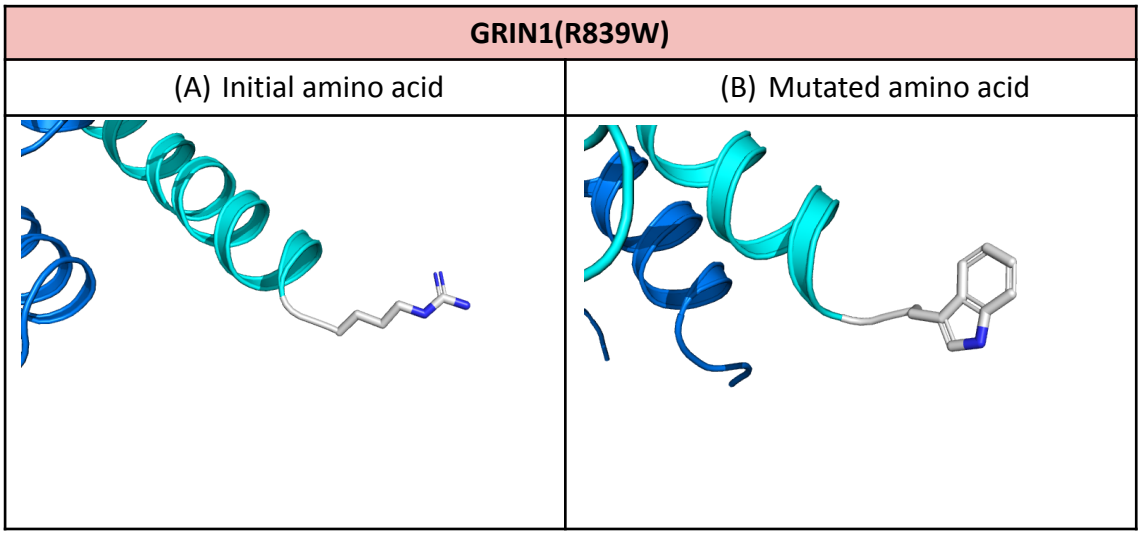

Figure 7: GRIN1(R839W) variant in NMDA receptor molecular model. (A): Initial amino acid. (B): Mutated amino acid. GRIN1 is coloured in cyan, GRIN2A in light-blue, and GRIN2B in marine.

Last GRIN1 variant GRIN1(R839W) seen at Figure 7, is located at the extreme of the GRIN1 chain. In fact, it is the last position hold by the NMDA molecular model. The change of an arginine (basic amino acid) for a tryptophan (neutral aromatic) confers an aromatic ring at the extreme of the GRIN1 sequence. However, it is not a critical change, as both arginine and tryptophan interact with the same atoms within 4Å. Due to the position of the mutation, this variant could be interacting with the CTD domain.

GRIN2A(C456R)	
(A) Initial amino acid	(B) Mutated amino acid
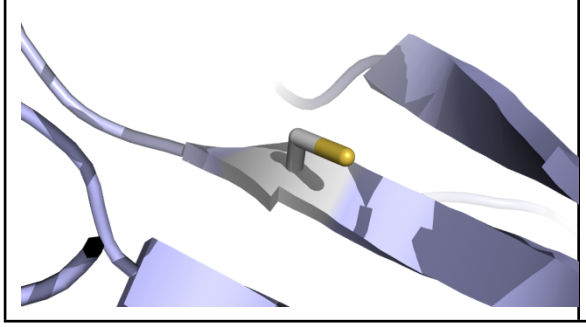	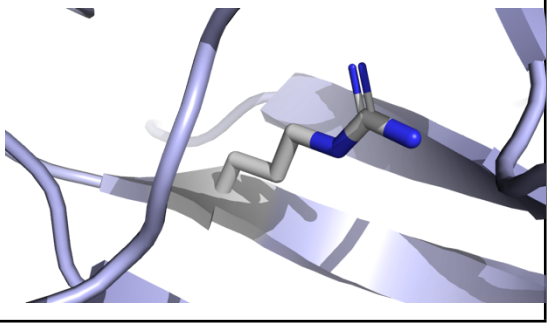

Figure 8: GRIN2A(C456R) variant in NMDA receptor molecular model. (A): Initial amino acid. (B): Mutated amino acid. GRIN1 is coloured in cyan, GRIN2A in light-blue, and GRIN2B in marine.

The first GRIN2A variant, GRIN2A(C456R), is located at the ligand binding domain. Changing a neutral and polar cysteine for a basic arginine (Figure 8) grants the position with a larger side-chain, interacting then with more atoms within 4Å. This larger side-chain could interfere the binding of glutamate or glycine.

GRIN2A(G644S)	
(A) Initial amino acid	(B) Mutated amino acid
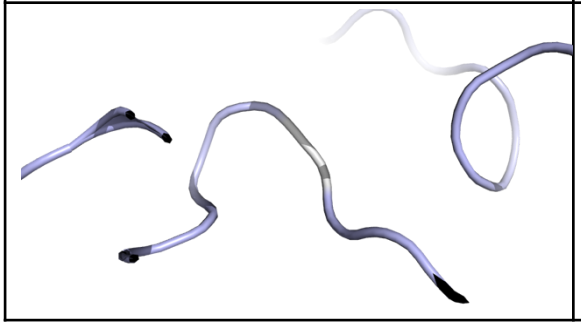	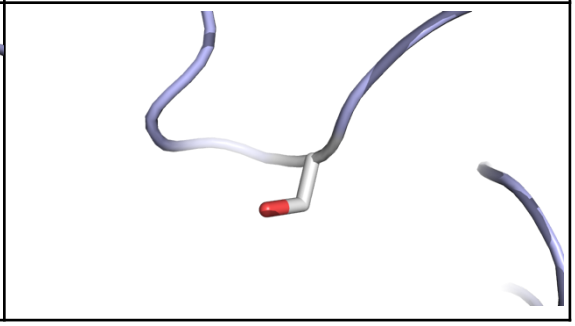

Figure 9: GRIN2A(G644S) variant in NMDA receptor molecular model. (A): Initial amino acid. (B): Mutated amino acid. GRIN1 is coloured in cyan, GRIN2A in light-blue, and GRIN2B in marine.

Second GRIN2A variant, GRIN2A(G644S), changes an apolar glycine for a polar serine (see Figure 9). However, as the serine has not a vast side chain, they both interact with the same atoms within 4Å. It is located at the transmembrane domain so it could cause problems with the correct formation of the receptor.

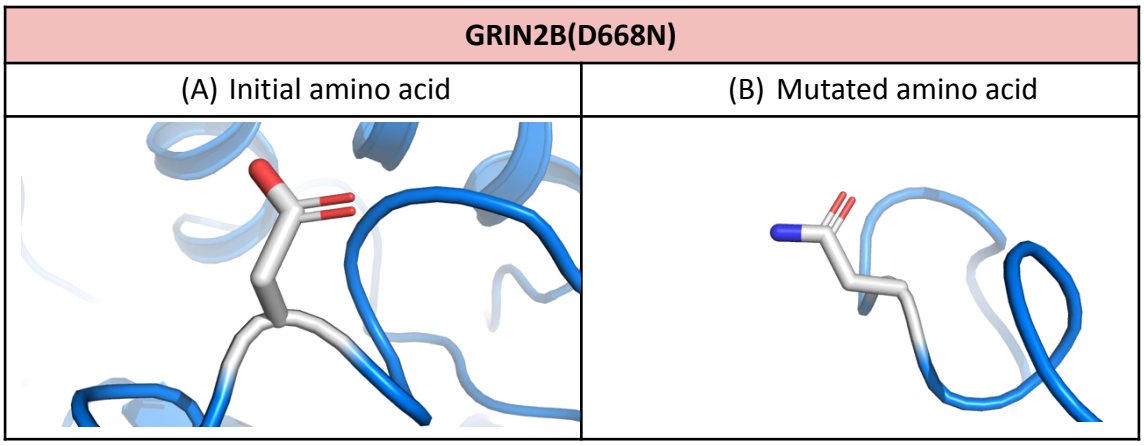

Figure 10: GRIN2B(D668N) variant in NMDA receptor molecular model. (A): Initial amino acid. (B): Mutated amino acid. GRIN1 is coloured in cyan, GRIN2A in light-blue, and GRIN2B in marine.

When it comes to GRIN2B variants, first one GRIN2B(D668N) is located at the transmembrane domain. It produces the change of an aspartic acid for an asparagine (Figure 10), as they have a similar side-chain structure, the change does not imply the interaction with more atoms within 4Å. However, this amino acid change could interfere in the correct formation of the receptor as the TMD is a really sensitive are to molecular changes.

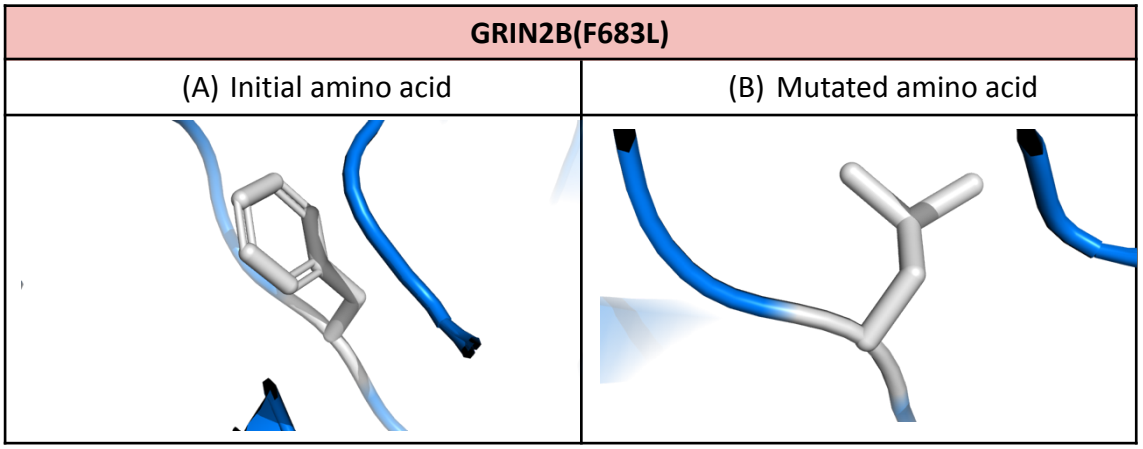

Figure 11: GRIN2B(F683L) variant in NMDA receptor molecular model. (A): Initial amino acid. (B): Mutated amino acid. GRIN1 is coloured in cyan, GRIN2A in light-blue, and GRIN2B in marine.

Then, GRIN2B(F683L) variant is located in the ligand binding domain. In this case, an aromatic phenylalanine is mutated into a leucine, as shown in Figure 11, thus deleting the aromatic ring causing a decrement on the number of interactions between atoms within 4Å.The functional evaluation of GluN subunits variants expression in cell lines of this variant shows a correct formation and surface expression. So it can be determined that the amino acid change does not provoke a malformation of the receptor. However,

as it is located in the LBD, it could possibly cause a loss of function. Even though, more assays should be performed to ensure and have severe outcomes.

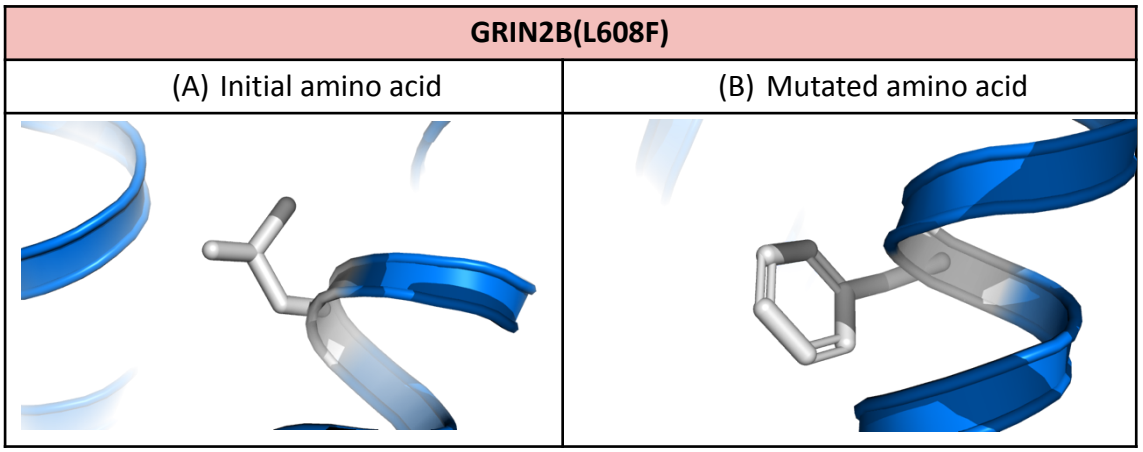

Figure 12: GRIN2B(L608F) variant in NMDA receptor molecular model. (A): Initial amino acid. (B): Mutated amino acid. GRIN1 is coloured in cyan, GRIN2A in light-blue, and GRIN2B in marine.

On the contrary to GRIN2B(F683L) variant, GRIN2B(L608F) introduces an aromatic phenylalanine in the place of a leucine, represented in Figure 12. This mutation located in the transmembrane domain increases the number of interactions between atoms within 4Å. In the original sequence, the leucine interacts with just a tryptophan and two leucines, at positions 607, 609 and 612, respectively. However, the mutation causes an interaction with an alanine at position 605, and an isoleucine at position 606, apart from the tryptophan and two leucines, at positions 607, 609 and 612, respectively. As this mutation is in the domain where the channel pore is located, and it gives a larger side-chain to the 608 position, the channel pore could be affected. As the functional evaluation of GluN subunits variants expression in cell lines indicated this concrete variant had a correct formation and surface expression, there is a high likelihood that this amino acid change could interfere the binding of magnesium, thus causing a gain of function; as the possibility of loss of function because of malformation of the receptor is discarded due to immunofluorescence assay shows clear surface expression of the receptor.

GRIN2B(I641T)	
(A) Initial amino acid	(B) Mutated amino acid
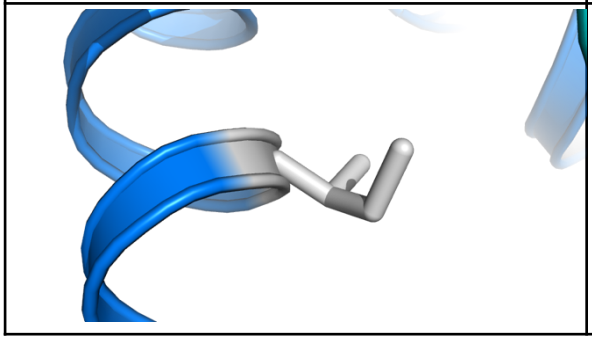	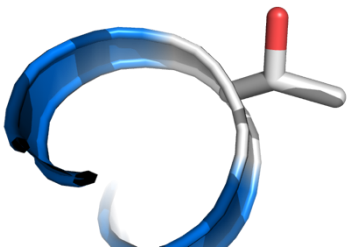

Figure 13: GRIN2B(I641T) variant in NMDA receptor molecular model. (A): Initial amino acid. (B): Mutated amino acid. GRIN1 is coloured in cyan, GRIN2A in light-blue, and GRIN2B in marine.

Finally, the last variant analysed GRIN2B(I641T), that is also located in the transmembrane domain. Here a change of an apolar isoleucine for a polar threonine is faced (see Figure 13). As it seems to be a critical change for the structure of the domain, in fact both amino acids interact with the same atoms within 4Å. In spite of that, the as the channel pore is a really sensitive area it could evenly be affected.

4.4- Molecular mapping of NMDA receptor mutants

All the functional and pathogenic data from GRINdb and GenomAD was integrated in the triheteromeric molecular model of the NMDA receptor (GluN1)2- GluN2A-GluN2B, so as to map all the mutated positions in order to determinate the regions affected by most pathogenic variants. As well as which domains are more susceptible to be causing a gain or loss of function

In order to know quantitatively how many variants had to be mapped, a quantitative analysis for the three *GRIN* genes was performed, and the global result is exposed at Table 7.

In this project just missense variants have been analyzed, indicating a homogenous distribution of the number of variants in the 3 genes. Even though GRIN2A has the higher number of missense variants, it is not a significative difference. When it comes to pathogenicity, the 3 genes show a higher number of neutral mutations than disease-associated mutations. And even a lower value of uncertain pathogenesis variants. Thus, indicating that not all *GRIN* mutations cause a pathological condition.

Regarding variants classified according to their functionality, as it had been previously seen in the molecular model variants mapping, there is a higher number of LoF than GoF mutations. That's because if a variants interferes the binding of neurotransmittors it will provoke a LoF, as well as if it produces a malformation of the receptor, causing also a LoF.

Table 7: Quantitative analysis of missense variants, pathogenicity, and functionality.

	Missense variants	Pathogenicity			Functionality		
		Neutral	Disease-associated	Uncertain pathogenesis	GoF	LoF	Complex
GRIN1	343	236	85	22	1	18	7
GRIN2A	837	640	132	65	4	31	3
GRIN2B	628	446	127	55	1	51	6
Total	1808	1322	344	142	6	100	16

When the determinate number of variants was quantifies, all the functional and pathogenic information on *GRIN* missense variants was integrated into the NMDA receptor structure, resulting in 2 different structures according to their pathogenicity and functionality were generated.

***GRIN* variants pathogenicity**

GRIN variants pathogenicity is classified as "Disease-associated," "Neutral," or "Uncertain pathogenicity," according to their NMDAR alteration.

Figure 14 shows the pathogenicity of all the mutated amino acids in the NMDA receptor structure, being neutral variants coloured in green, disease-associated in red, and those with an uncertain pathogenesis in orange.

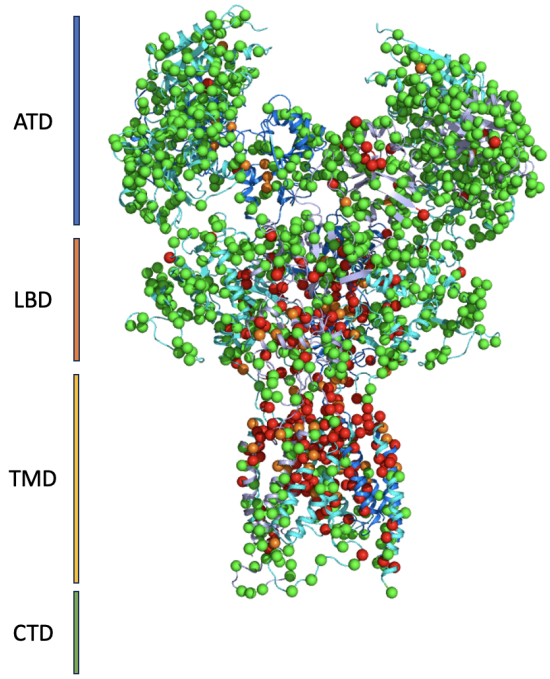

Figure 14: Pathogenicity of *GRIN* variants *in* NMDAr structure. The molecular model shows GRIN1 coloured in cyan, GRIN2A in light-blue, and GRIN2B in marine. Neutral variants (green), disease-associated (red) and uncertain pathogenesis (orange).

Observing the pathogenicity of the variants in the receptor structure, it can be determined that the extracellular domains, ATD and LBD, suffer less pathogenic variants than the TMD. This is because these regions tolerate mutations without affecting the structure and function of the NMDA receptor. In addition, the ATD suffers a lower number of disease-associated variants than the LBD. When it comes to LBD, at the inner part of the receptor and in the glutamate/glycine binding site, more disease-associated variants are reported; owing to the fact that these regions are essential to maintain the binding of the neurotransmitters, as well as to transduce the response to the channel pore. The transmembrane domain is an area really influenced by disease-associated mutations, especially in the upper region and around the magnesium binding site. Amino acid changes are less tolerated at these regions, because they are essential to maintain the open of the channel and the magnesium blockage.

***GRIN* variants functionality**

When it comes to disease-associated *GRIN* variants, they are classified according to their NMDA receptor misfunction. Gain of Function (GoF) mutations facilitate NMDAR signalling, in contrast to Loss of Function (LoF) variants which decrease the activity of the receptor causing a hypoglutamatergic function. The image below (Figure 15) shows the different *GRIN* variants mapped in the triheteromeric molecular model of the NMDA receptor according to their functionality.

In addition, GoF and LoF variants are presented in different molecular model images (Figure 16-A and figure 16-B, respectively) to appreciate the areas they are most present and causing NMDAr malfunction.

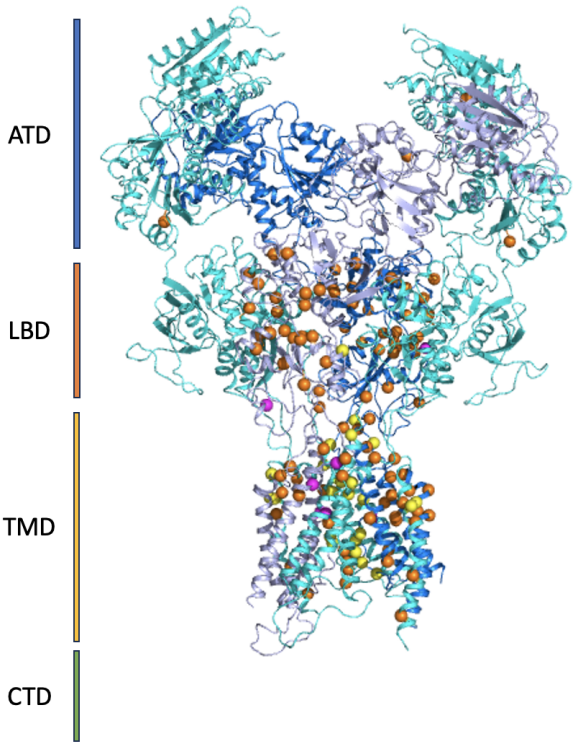

Figure 15: Functionality of *GRIN* variants in NMDAr structure. The molecular model shows GRIN1 coloured in cyan, GRIN2A in light-blue, and GRIN2B in marine. Neutral variants (green), disease-associated (red) and complex (orange). Gain of Function (GoF) variants are coloured in magenta, Loss of Function (LoF) in orange, and complex mutations in yellow.

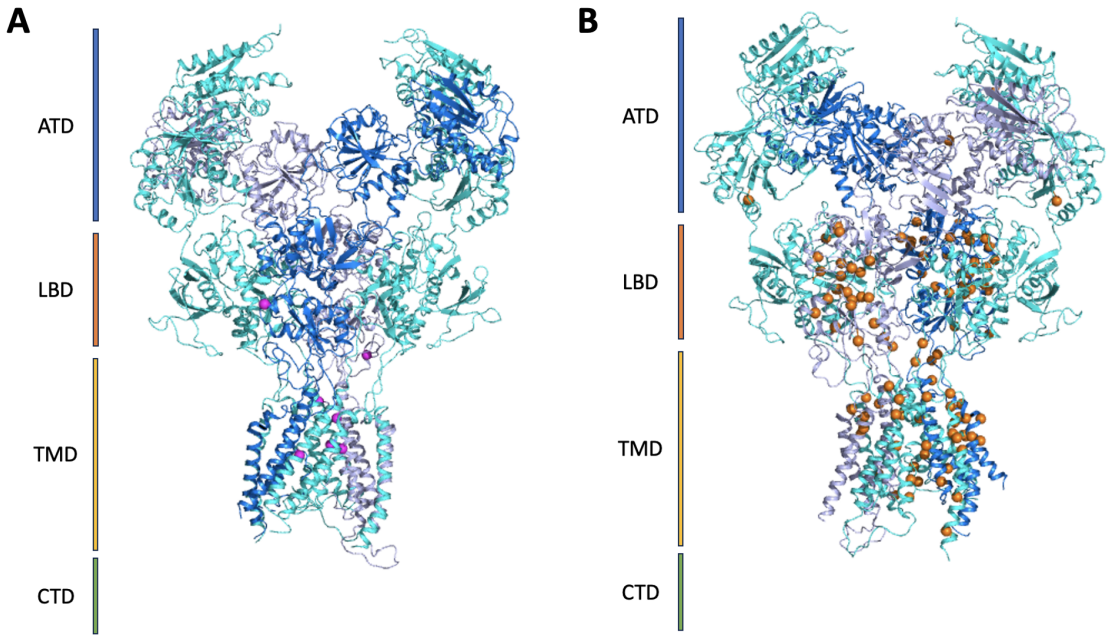

Figure 16: GoF and LoF *GRIN* variants in NMDAr structure. (A): GoF variants colured in magenta. (B): LoF variants coloured in orange. The molecular model shows GRIN1 coloured in cyan, GRIN2A in light-blue, and GRIN2B in marine.

Once having mapped and quantified the *GRIN* variants according to their functionality, it can be determined that GoF variants are mainly located at the TMD. That makes sense since at the TMD is located the magnesium binding site to block the receptor at resting membrane potential. If there is an alteration in that area, it will interfere in the binding of magnesium thus causing the constant state of the open receptor, resulting in a gain of function.

On contrast, LoF variants located at the LBD interfere in the binding of glutamate and glycine. If the neurotransmitters cannot bind to the receptor, it results in a loss of function. Moreover, there is also presence of LoF mutations in the TMD, being a really sensitive area to alterations being able to disrupt the NMDAr formation. If a mutation inhibits the correct formation and folding of the receptor, it will conclude in a loss of function.

5- CONCLUSIONS

From the 10 original de novo missense variants, 6 DNAs carrying the desired mutation were synthesized.

Variants GRIN2B(L608F), GRIN2B(F683L), and GRIN1(R844C), tested with western blot and immunofluorescence assays showing correct formation and expression of NMDA receptor. Variant GRIN2B(F683L) is located at the LBD and could interfere the binding of the neurotransmitters. GRIN2B(L608F) is located at the TMD, is really likely to cause a gain of function, as it does not disturb the NMDA receptor formation. Despite those resolutions, western blot and immunofluorescence assays should be repeated to ensure severe and trustful results.

Variants conferring a larger side-chain at the TMD, as GRIN1(D658Y) and GRIN2B(L608F), could cause a receptor malformation (LoF) or interfere in the magneiusm blockage (GoF). An amino acid change with similar side-chain structures, like GRIN1(G638A) and GRIN2B(D668N), may not interfere the NMDA receptor function. The change of a polar for an apolar amino acid, or inversely, as GRIN2B(I641T) and GRIN2A(G644S), could cause a pathogenic condition. Mutations conferring larger side-chains, like GRIN2A(C456R), at the LBD couls interfere the binding of glutamate.
Finally, variants affecting the most external part, including GRIN1(R839W) and GRIN1(R844C), could interact with the CTD causing an uncertain pathogenesis mutation.

Once all the pathogenic and functional data was integrated in the triheteromeric molecular model of the NMDA receptor, some regions seem to be more affected by disease-associated variants.Pathogenic variants mainly affect the LBD and TMD. The LBD is mostly affected by LoF variants, because they may interfere in the binding of glutamate and glycine. Whereas the TMD is affected by both GoF, interfering in the magnesium blockage, and LoF, causing a malformation of the receptor.

Finally, quantitative analysis shows missense variants are distributed through the whole receptor homogeneously, and there is a higher number of LoF mutations.

6- REFERENCES

Binder, M., Hirokawa, N., & Windhorst, U. (2009). *Encyclopedia of neuroscience*. http://www.rybak-et-al.net/pdfs/Rybak%20and%20Smith%202009.pdf

Chemical Analysis, Life Sciences, and Diagnostics | Agilent. (n.d.). Retrieved May 31, 2023, from https://www.agilent.com/

Choi, D. W., Maulucci-Gedde, M., & Kriegstein, A. R. (1987). Glutamate neurotoxicity in cortical cell culture. *Soc Neuroscience*, *7*(2), 357–388. https://www.jneurosci.org/content/7/2/357.short

Chou, T., Tajima, N., Cell, A. R.-H.-, & 2020, undefined. (n.d.). Structural basis of functional transitions in mammalian NMDA receptors. *Elsevier*. Retrieved May 31, 2023, from https://www.sciencedirect.com/science/article/pii/S0092867420306851

García-Recio, A., Santos-Gómez, A., Soto, D., Julia-Palacios, N., García-Cazorla, À., Altafaj, X., & Olivella, M. (2021). GRIN database: A unified and manually curated repertoire of GRIN variants. *Human Mutation*, *42*(1), 8–18. https://doi.org/10.1002/HUMU.24141

Gegelashvili, G., pharmacology, A. S.-M., & 1997, undefined. (n.d.). High affinity glutamate transporters: regulation of expression and activity. *ASPET*. Retrieved May 31, 2023, from https://molpharm.aspetjournals.org/content/52/1/6.short

Gregory, K., Noetzel, M., biology, C. N.-P. in molecular, & 2013, undefined. (n.d.). Pharmacology of metabotropic glutamate receptor allosteric modulators: structural basis and therapeutic potential for CNS disorders. *Elsevier*. Retrieved May 31, 2023, from https://www.sciencedirect.com/science/article/pii/B9780123945877000026

Hansen, K., Yi, F., Perszyk, R., … H. F.-J. of G., & 2018, undefined. (n.d.). Structure, function, and allosteric modulation of NMDA receptors. *Rupress.Org*. Retrieved May 31, 2023, from https://rupress.org/jgp/article-abstract/150/8/1081/43759

Johnson, J., Nature, P. A.-, & 1987, undefined. (n.d.). Glycine potentiates the NMDA response in cultured mouse brain neurons. *Nature.Com*. Retrieved May 31, 2023, from https://www.nature.com/articles/325529a0

Kantrowitz, J., bulletin, D. J.-B. research, & 2010, undefined. (n.d.). N-methyl-d-aspartate (NMDA) receptor dysfunction or dysregulation: the final common pathway on the road to schizophrenia? *Elsevier*. Retrieved May 31, 2023, from https://www.sciencedirect.com/science/article/pii/S0361923010000870

Karakas, E., & Furukawa, H. (2014). Crystal structure of a heterotetrameric NMDA receptor ion channel. *Science*, *344*(6187), 992–997. https://doi.org/10.1126/SCIENCE.1251915

Krivov, G. G., Shapovalov, M. V., & Dunbrack, R. L. (2009). Improved prediction of protein side-chain conformations with SCWRL4. *Proteins: Structure, Function and Bioinformatics*, *77*(4), 778–795. https://doi.org/10.1002/PROT.22488

Lunin, V. Y., Urzhumtsev, A., Bockmayr, A., Fokin, A., Urzhumtsev, A., Afonine, P., Lunin, V. Y., Harding, M., Turkenburg, M., Ballard, C., & Howard-Eales, M. (n.d.). Pymol: An open-source molecular graphics tool. *Citeseer*. Retrieved May 31, 2023, from https://citeseerx.ist.psu.edu/document?repid=rep1&type=pdf&doi=ab82608e9a44c17b60d7f908565fba628295dc72#page=44

Oligos, DNA / RNA Synthesis - biomers.net Oligonucleotides. (n.d.). Retrieved May 31, 2023, from https://www.biomers.net/

Rivadulla, C., Sharma, J., Neuroscience, M. S.-J. of, & 2001, undefined. (2001). Specific roles of NMDA and AMPA receptors in direction-selective and spatial phase-selective responses in visual cortex. *Soc Neuroscience*. https://www.jneurosci.org/content/21/5/1710.short

Rojas, H., Neurociencias, I. N.-A. de, & 2017, undefined. (2016). Glutamato para principiantes. *Medigraphic.Com*, *21*(3). https://www.medigraphic.com/cgi-bin/new/resumen.cgi?IDARTICULO=72362

Rossum, G. Van, & Drake, F. (2009). *Introduction to python 3: python documentation manual part 1*. https://dl.acm.org/doi/abs/10.5555/1592885

Santos-Gómez, A., Miguez-Cabello, F., García-Recio, A., Locubiche-Serra, S., García-Díaz, R., Soto-Insuga, V., Guerrero-López, R., Juliá-Palacios, N., Ciruela, F., García-Cazorla, À., Soto, D., Olivella, M., & Altafaj, X. (2020). Disease-associated GRIN protein truncating variants trigger NMDA receptor loss-of-function. *Academic.Oup.Com*, *29*(24), 3859–3871. https://doi.org/10.1093/hmg/ddaa220

Schackert, F. K., Biedermann, J., Abdolvand, S., Minniberger, S., Song, C., Plested, A. J. R., Carloni, P., & Sun, H. (2023). Mechanism of Calcium Permeation in a Glutamate Receptor Ion Channel. *Journal of Chemical Information and Modeling*, *63*(4), 1293–1300. https://doi.org/10.1021/ACS.JCIM.2C01494

Soto, D., Olivella, M., Grau, C., Armstrong, J., Alcon, C., Gasull, X., Santos-Gómez, A., Locubiche, S., De Salazar, M. G., García-Díaz, R., Gratacòs-Batlle, E., Ramos-Vicente, D., Chu-Van, E., Colsch, B., Fernández-Dueñas, V., Ciruela, F., Bayés, À., Sindreu, C., López-Sala, A., … Altafaj, X. (2019). L-Serine dietary supplementation is associated with clinical improvement of loss-of-function GRIN2B-related pediatric encephalopathy. *Science Signaling*, *12*(586). https://doi.org/10.1126/SCISIGNAL.AAW0936

Szepetowski, P., Kristensen, A. S., Mao, X., Altafaj, X., Olivella, M., Santos-Gómez, A., García-Recio, A., Miguez-Cabello, F., & Soto, D. (2022). Identification of homologous GluN subunits variants accelerates GRIN variants stratification. *Ncbi.Nlm.Nih.Gov*. https://doi.org/10.3389/fncel.2022.998719

Thomas, S., aging, G. G.-C. interventions in, & 2009, undefined. (2009). Memantine: a review of studies into its safety and efficacy in treating Alzheimer's disease and other dementias. *Taylor & Francis*, 367. https://doi.org/10.2147/cia.s6666

Webb, B., & Sali, A. (2016). Comparative protein structure modeling using MODELLER. *Current Protocols in Bioinformatics*, *2016*, 5.6.1-5.6.37. https://doi.org/10.1002/CPBI.3

Willard, S. S., & Koochekpour, S. (2013). Glutamate, Glutamate Receptors, and Downstream Signaling Pathways. *International Journal of Biological Sciences*, *9*(9), 948. https://doi.org/10.7150/IJBS.6426

Zhang, J., Chang, S., Xu, P., Miao, M., Wu, H., Reports, Y. Z.-C., & 2018, undefined. (n.d.). Structural basis of the proton sensitivity of human GluN1-GluN2A NMDA receptors. *Elsevier*. Retrieved May 31, 2023, from https://www.sciencedirect.com/science/article/pii/S2211124718318473

SUPPLEMENTARY MATERIAL

GitHub link for python scripts: https://github.com/ismaelveramu/TFG-Ismael

Images of the interaction of correct and mutated amino acids within 4Å for each mutation.

GRIN1(D658Y)	
Atoms within 4Å of correct amino acid	Atoms within 4Å of mutated amino acid
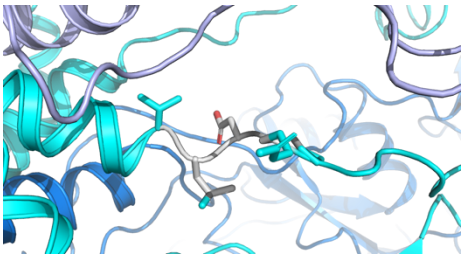	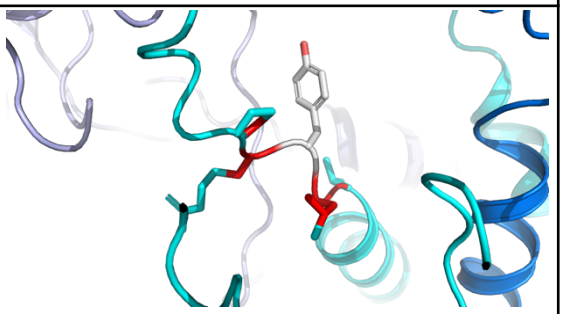

GRIN1(G638A)	
Atoms within 4Å of correct amino acid	Atoms within 4Å of mutated amino acid
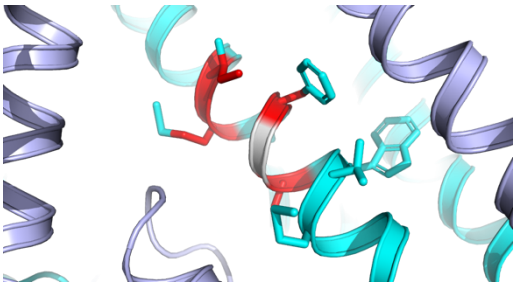	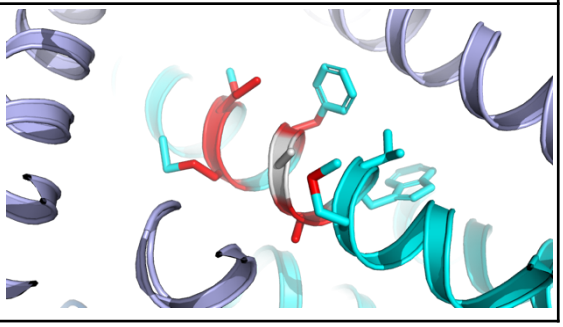

GRIN1(R839W)	
Atoms within 4Å of correct amino acid	Atoms within 4Å of mutated amino acid
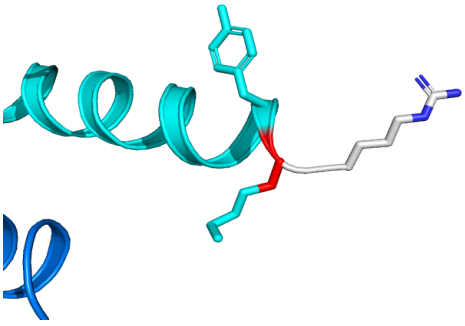	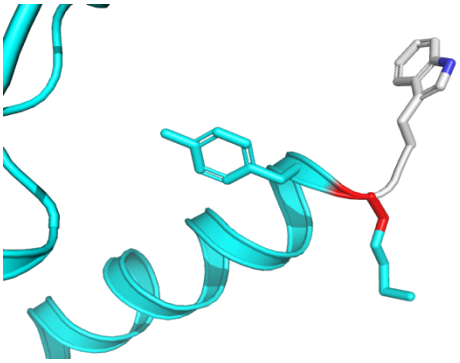

GRIN2A(C456R)	
Atoms within 4Å of correct amino acid	Atoms within 4Å of mutated amino acid
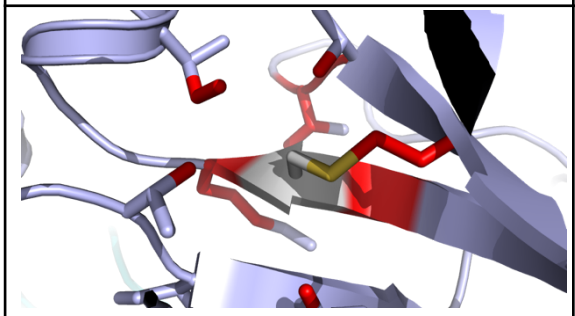	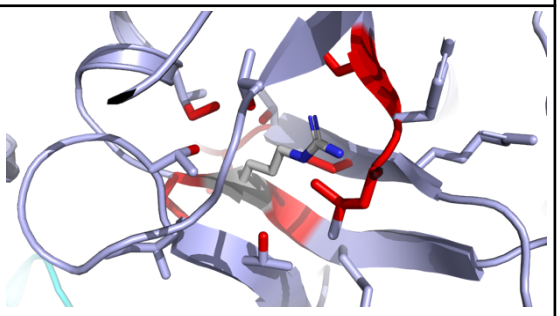

GRIN2A(G644S)	
Atoms within 4Å of correct amino acid	Atoms within 4Å of mutated amino acid
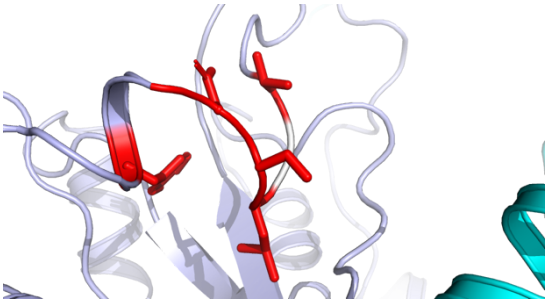	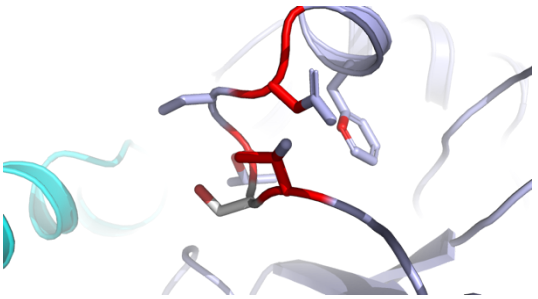

GRIN2B(D668N)	
Atoms within 4Å of correct amino acid	Atoms within 4Å of mutated amino acid
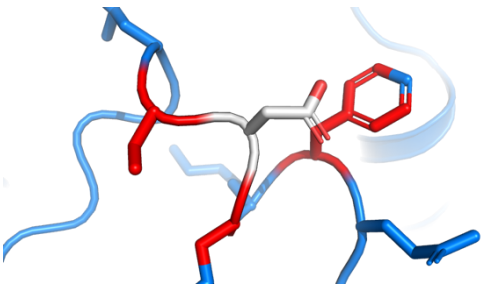	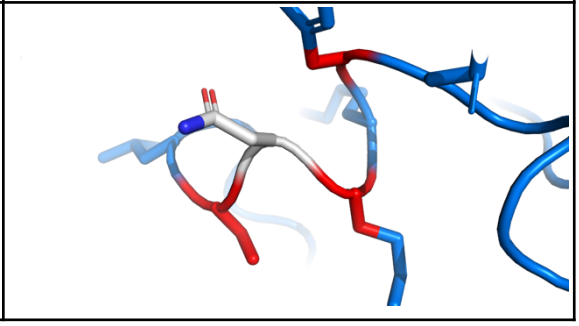

GRIN2B(F683L)	
Atoms within 4Å of correct amino acid	Atoms within 4Å of mutated amino acid
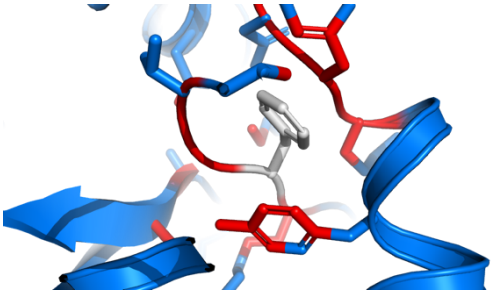	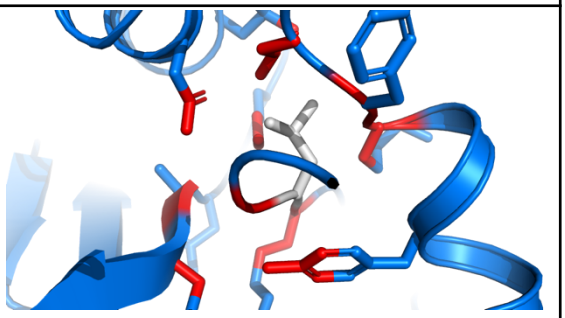

GRIN2B(L608F)	
Atoms within 4Å of correct amino acid	Atoms within 4Å of mutated amino acid
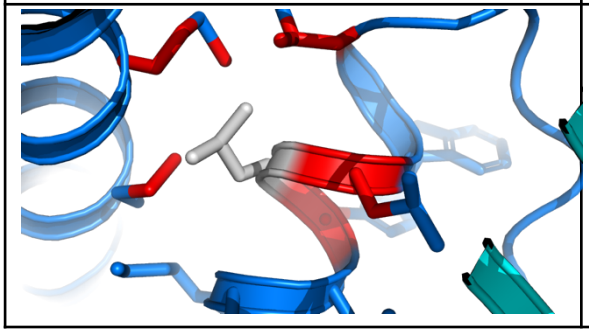	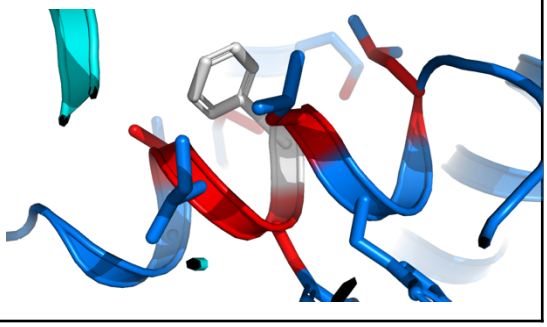

GRIN2B(I641T)	
Atoms within 4Å of correct amino acid	Atoms within 4Å of mutated amino acid